MASAGA: A Stochastic Algorithm for Manifold Optimization

Reza Babanezhad, Issam H. Laradji, Alireza Shafaei, and Mark Schmidt

Department of Computer Science, University of British Columbia
Vancouver, British Columbia, Canada
{rezababa,issamou,shafaei,schmidtm}@cs.ubc.ca

Abstract. We consider the stochastic optimization of finite sums where the functions are smooth and convex on a Riemannian manifold. We present MASAGA, an extension of SAGA on Riemannian manifolds. SAGA is a variance reduction technique that often performs faster in practice compared to methods that rely on updating the expensive full gradient frequently such as SVRG. However, SAGA typically requires extra memory proportional to the size of the dataset to store stale gradients. This memory footprint can be reduced when the gradient vectors have a structure such as sparsity. We show that MASAGA achieves a linear convergence rate when the objective function is smooth, convex, and lies on a Riemannian manifold. Furthermore, we show that MASAGA achieves faster convergence rate with non-uniform sampling than the uniform sampling. Our experiments show that MASAGA is faster than the RSGD algorithm for finding the leading eigenvector corresponding to the maximum eigenvalue.

Keywords: Variance Reduced Stochastic Optimization· Riemannian Manifold.

1 Introduction

The most common supervised learning methods in machine learning use empirical risk minimization during the training. The minimization problem can be expressed as minimizing a finite sum of loss functions evaluated at a single data sample. We consider the problem of minimizing a finite sum over a Riemannian manifold:

$$\min_{x \in \mathcal{X} \subset \mathcal{M}} f(x) = \frac{1}{n} \sum_{i=1}^{n} f_i(x),$$

where $\mathcal{X}$ is a geodesically convex set in the Riemannian manifold $\mathcal{M}$. Each function f_i is geodesically Lipschitz smooth and the sum is geodesically strongly convex over the set $\mathcal{X}$. Learning of several machine learning models can be written as an optimization over a Riemannian manifold. Principal component analysis (PCA) [38], dictionary learning [32], Gaussian mixture model (GMM) [10], covariance estimation [35], and computing the Riemannian centroid [11] are a few of such models.

When $\mathcal{M} = \mathbb{R}^d$, the problem reduces to convex optimization in Euclidean space. An extensive body of literature studies this problem in deterministic and stochastic settings [5,28,21,27,22]. It is possible to convert the optimization over a manifold into an optimization in Euclidean space by adding $x \in \mathcal{X}$ as an optimization constraint. The problem could be treated as an optimization in Euclidean space with an extra projection step. However, the problem with this approach is that we are not explicitly exploiting the geometrical structure of the manifold. Furthermore, the projection step for manifolds such as positive-definite matrices could be quite expensive. Finally, a function could be non-convex in Euclidean space, but geodesically convex over an appropriate manifold. With geodesic convexity, an optimization over the manifold could converge as fast as convex optimization in Euclidean space.

Stochastic optimization over manifolds and their convergence properties have received significant interest in the recent literature [4,37,14,29,36]. Bonnabel [4] and Zhang *et al*. [37] analyze the application of

SGD for optimization over manifolds. Similar to Euclidean space optimization with SGD, these methods suffer from the aggregating variance problem [39]. Therefore, the analysis of these methods gets a sublinear convergence rate similar to vanilla SGD. Variance reduction techniques have been introduced to diminish the variance in SGD analysis of finite sums over linear spaces. The variance reduction techniques can be categorized into two groups: (i) memory based approaches such as SAG [16], SAGA [6], and SDCA [31], and (ii) full gradient based approaches such as SVRG [12] and its variants [19,15,24]. Memory based methods use the memory to store a stale gradient of each f_i. Roughly, during each iteration, they pick a random f_i and evaluate its gradient and update the corresponding memory slot with the new value. Then, they use the average of stored values as an approximate gradient of f. In contrast, full gradient based methods only store the gradient of f, and not the individual f_i's. These methods occasionally evaluate and update the gradient of f and use it to approximate the full gradient during each iteration.

Several methods [14,29,36] use SVRG to optimize the finite sum problem over a Riemannian manifold. Similar to the linear space analysis, these methods converge linearly for geodesically Lipschitz smooth and strongly convex functions. However, these methods require an extra full gradient evaluation just like the original SVRG. Although SVRG often dramatically outperforms the classical gradient descent (GD) and SGD, the extra gradient evaluation typically yields a slower convergence than memory based methods. Furthermore, the extra gradient calculations of SVRG makes it even slower than the classical SGD during the early iterations where SGD has the most advantage [9]. When the bottleneck of the process is the gradient computation itself, using memory based methods is more advantageous [7,3].

We present *MASAGA*, a SAGA [6] based algorithm to optimize finite sums over Riemannian manifolds. MASAGA needs memory in the order of the dataset size to approximate the full gradient. This memory requirement could be alleviated when the gradient of each f_i admits a special structure such as sparsity [30,34]. We analyze MASAGA and present a proof of linear convergence for geodesically strongly convex functions similar to the SVRG based counterparts [14,29,36]. We also show in theory that both MASAGA and RSVRG [36] with a non-uniform sampling strategy can converge faster than the uniform sampling scheme. Finally, we consider the problem of finding the leading eigenvector that minimizes a quadratic function over a sphere. We show that MASAGA converges linearly with uniform and non-uniform sampling schemes on this problem. For evaluation, we consider one synthetic and two real datasets. The real datasets are MNIST [17] and Ocean data [18]. We find the leading eigenvector of each class and visualize the results. On MNIST, the leading eigenvectors resemble the images of each digit class, whereas, for the Ocean dataset, we observe that the leading eigenvector represents the background image in the dataset.

In section 2, we present an overview of the essential concepts in Riemannian geometry. We define the geodesically convex and smooth function classes based on Zhang *et al*. [37]. We also briefly review the original SAGA algorithm. In section 3, we introduce MASAGA algorithm and analyze its convergence. We show that with a non-uniform sampling scheme MASAGA converges faster than uniform sampling. Finally, in section 4, we empirically verify the theoretical linear convergence results.

2 Preliminaries

In this section, we first review concepts related to the Riemannian manifold. Then, we introduce the class of functions that we optimize over the manifold. Finally, we briefly review the original SAGA algorithm.

2.1 Riemannian Manifold

In this section, we review the basic and fundamental concepts of Riemannian manifold and geometry. For a more detailed review we refer the interested reader to the literature [26,1,33]. Throughout the paper, we use manifold and Riemannian manifold exchangeably.

A Riemannian manifold denoted by $(\mathcal{M}, G)$ is a smooth manifold over $\mathbb{R}^d$, and G is its metric. At any point x in the manifold $\mathcal{M}$, we define $\mathcal{T}_{\mathcal{M}}(x)$ to be the tangent plane of that point, and G defines an inner product in this plane. Formally let p and q be two vectors in $\mathcal{T}_{\mathcal{M}}(x)$, then $\langle p, q \rangle_x = G(p, q)$. Similar to Euclidean space, using G we can define the norm of a vector and the angle between two vectors.

To measure the distance between two points on the manifold, we use the geodesic distance. Geodesics on the manifold generalize the concept of straight lines in Euclidean space. Let us denote the geodesic with $\gamma(t) : [0, 1] \to \mathcal{M}$, that is a function with constant gradient *i.e.*,

$$\frac{d^2}{dt^2}\gamma(t) = 0.$$

To map a point in $\mathcal{T}_{\mathcal{M}}(x)$ to $\mathcal{M}$, we use the Exponential function $\mathrm{Exp}_x : \mathcal{T}_{\mathcal{M}}(x) \to \mathcal{M}$. If $\mathrm{Exp}_x(p) = z$, meaning that there is a geodesic curve $\gamma_x^z(t)$ on the manifold such that it starts from x *i.e.*, $\gamma_x^z(0) = x$ and ends at z *i.e.*, $\gamma_x^z(1) = z$ and its velocity is p *i.e.*, $\frac{d}{dt}\gamma_x^z(0) = p$.

$$\mathrm{Exp}_x(p) = \gamma_x^z(1).$$

When the Exp function is defined for every point in the manifold, we call the manifold geodesically complete. For example, the unit sphere in $\mathcal{R}^n$ is geodesically complete. If there is a unique geodesic curve between any two points in $\mathcal{M}' \in \mathcal{M}$, then the Exp_x function has an inverse defined by the Log function. Formally $\mathrm{Log}_x \equiv \mathrm{Exp}_x^{-1} : \mathcal{M}' \to \mathcal{T}_{\mathcal{M}}(x)$ and maps a point from $\mathcal{M}'$ back into the tangent plane at x. Moreover, the geodesic distance between x and z is the length of the unique shortest path between z and x and is equal to $\|\mathrm{Log}_x(z)\| = \|\mathrm{Log}_z(x)\|$.

Let $u, v \in \mathcal{T}_{\mathcal{M}}(x)$ be linearly independent so they specify a two dimensional subspace $\mathcal{S}_x \in \mathcal{T}_{\mathcal{M}}(x)$. The exponential map of this subspace $\mathrm{Exp}_x(\mathcal{S}_x) = \mathcal{S}_{\mathcal{M}}$ is a two dimensional submanifold in $\mathcal{M}$. The sectional curvature of S_M denoted by $\mathrm{K}(\mathcal{S}_{\mathcal{M}}, x)$ is defined as a Gauss curvature of S_M at x [40]. This sectional curvature helps us in the convergence analysis of the optimization method. The following lemma gives a trigonometric distance bound the and is essential for our analysis.

Lemma 1. *(Lemma 5 in [37]) Let a, b, and c be the side lengths of a geodesic triangle in a manifold with sectional curvature lower bounded by $K_{\min}$. Then*

$$a^2 \leq \frac{c\sqrt{|K_{\min}|}}{\tanh(\sqrt{|K_{\min}|}c)}b^2 + c^2 - 2bc\cos(\measuredangle(b, c))$$

Another important map used in our algorithm is the parallel transport. It transfers a vector from a tangent plane to another tangent plane along a geodesic. This map denoted by $\Gamma_x^z : \mathcal{T}_{\mathcal{M}}(x) \to \mathcal{T}_{\mathcal{M}}(z)$, maps a vector from the tangent plane $\mathcal{T}_{\mathcal{M}}(x)$ to a vector in the tangent plane $\mathcal{T}_{\mathcal{M}}(z)$ while preserving the norm and inner product values.

$$\langle p, q \rangle_x = \langle \Gamma_x^z(p), \Gamma_x^z(q) \rangle_z$$

Grassmann manifold. Here we review the Grassmann manifold $\mathrm{Grass}(p, n)$ as a practical Riemannian manifold used in machine learning. Let p and n be positive integers and $p \leq n$. $\mathrm{Grass}(p, n)$ contains all orthogonal matrices in $\mathbb{R}^{n \times p}$, with orthonormal columns. Therefore if $M \in \mathrm{Grass}(p, n)$ then we have $M^\top M = I$, where $I \in \mathbb{R}^{p \times p}$ is the identity matrix. Let $q \in \mathcal{T}_{\mathrm{Grass}(p,n)}(x)$, and $q = U\Sigma V^\top$ be its p-rank singular value decomposition. Then we have:

$$\mathrm{Exp}_x(tq) = xV\cos(t\Sigma)V^\top + U\sin(t\Sigma)V^\top.$$

The parallel transport along a geodesic curve $\gamma(t)$ such that $\gamma(0) = x$ and $\gamma(1) = z$ is defined as:

$$\Gamma_x^z(tq) = (-xV\sin(t\Sigma)U^\top + U\cos(t\Sigma)U^\top + I - UU^\top)q.$$

2.2 Smoothness and Convexity on Manifold

In this section, we define convexity and smoothness of a function over a manifold following Zhang *et al*. [37]. We call $\mathcal{X} \in \mathcal{M}$ geodesically convex if for any two points $y, z \in \mathcal{X}$, there is a geodesic $\gamma(t)$ starting from y and ending in z with a curve inside of $\mathcal{X}$. For simplicity, we drop the subscript of inner product notation.

A function $f : \mathcal{X} \to \mathbb{R}$ is called geodesically convex if for any $y, z \in \mathcal{X}$ and the corresponding geodesic γ, for any $t \in [0, 1]$ we have:

$$f(\gamma(t)) \leq (1-t)f(y) + tf(z).$$

Similar to the Euclidean space, if the Log function is well defined we have the following definition for convex function:

$$f(z) + \langle g_z, \mathrm{Log}_z(y)\rangle \leq f(y),$$

where g_z is the subgradient of f at x. If f is a differentiable function, the Riemannian gradient of f at z is a vector g_z which satisfies $\frac{d}{dt}|_{t=0} f(\mathrm{Exp}_z(tg_z)) = \langle g_z, \nabla f(z)\rangle_z$, and ∇f is the gradient of f in $\mathbb{R}^n$. Furthermore, f is geodesically μ-strongly convex, if there is a μ such that:

$$f(z) + \langle g_z, \mathrm{Log}_z(y)\rangle + \frac{\mu}{2}\|\mathrm{Log}_z(y)\|^2 \leq f(y).$$

Let $x^* \in \mathcal{X}$ be the optimum of f *i.e.*, $g_{x^*} = 0$, then the following inequalities would hold

$$\|\mathrm{Log}_z(x^*)\|^2 \leq \frac{2}{\mu}(f(z) - f(x^*))$$
$$\langle g_z, \mathrm{Log}_z(x^*)\rangle + \frac{\mu}{2}\|\mathrm{Log}_z(x^*)\|^2 \leq 0$$

Finally, f is a geodesically Lipschitz smooth function with the parameter L, if it is differentiable over $\mathcal{M}$ and its gradient satisfies the following inequality:

$$\|g_z - \Gamma_y^z[g_y]\| \leq L\|\mathrm{Log}_z(y)\| = L\,\mathrm{d}(z, y),$$

where $\mathrm{d}(z, y)$ is the distance between z and y. Also, for a geodesically smooth f the following inequality holds:

$$f(y) \leq f(z) + \langle g_z, \mathrm{Log}_z(y)\rangle + \frac{L}{2}\|\mathrm{Log}_z(y)\|^2.$$

2.3 SAGA Algorithm

In this section we briefly review the SAGA method [6] and the assumptions associated with it. SAGA assumes f is μ-strongly convex, each f_i is convex, and each gradient f_i' is Lipschitz-continuous with the constant L. The method generates a sequence of iterates x_t using the SAGA Algorithm 1 (line 7). In the algorithm, M is the memory used to store stale gradients. During each iteration, SAGA picks one f_i randomly and evaluates its gradient at the current iterate value *i.e.*, $\nabla f_i(x_t)$. Next, it computes ν_t as the difference between the current $\nabla f_i(x_t)$ and the corresponding stale gradient of f_i stored in the memory plus the average

Algorithm 1 The Original SAGA Algorithm

1: **Input:** Learning rate η
2: Initialize $x_0 = 0$ and memory $M^{(0)}$ with gradient of x_0
3: **for** $t = 1, 2, 3, \dots$ **do**
4: $\quad \hat{\mu} = \frac{1}{n} \sum_{j=1}^{n} M^t[j]$
5: $\quad$ Pick i uniformly at random from $\{1 \dots n\}$
6: $\quad \nu_t = \nabla f_i(x_t) - M^t[i] + \frac{1}{n} \sum_{j=1}^{n} M^t[j]$
7: $\quad x_{t+1} = x_t - \eta(\nu_t)$
8: $\quad$ Set $M^{t+1}[i] = \nabla f_i(x_t)$ and $M^{t+1}[j] = M^t[j]$ for all $j \neq i$
9: **end for**

of all stale gradients (line 6). Then it uses this vector ν_t as an approximation of the full gradient and updates the current iterate similar to the gradient descent update rule. Finally, SAGA updates the stored gradient of f_i in the memory with the new value of $\nabla f_i(x_t)$.

Let $\rho_{\text{saga}} = \frac{\mu}{2(n\mu+L)}$. Defazio *et al.* [6] show that the iterate value x_t converges to the optimum x^* linearly with a contraction rate $1 - \rho_{\text{saga}}$, *i.e.*,

$$\mathbb{E}\left[\|x_t - x^*\|^2\right] \leq (1 - \rho_{\text{saga}})^t C,$$

where C is a positive constant.

3 Optimization on Manifold with SAGA

In this section we introduce the MASAGA algorithm (see Alg. 2). We make the following assumptions:

1. each f_i is geodesically L-Lipschitz continuous.
2. f is geodesically μ-strongly convex
3. f has an optimum in $\mathcal{X}$ *i.e.*, $x^* \in \mathcal{X}$
4. The diameter of $\mathcal{X}$ is bounded above, *i.e.*, $\max_{u,v \in \mathcal{X}} \mathrm{d}(u, v) \leq D$
5. Log_x is defined when $x \in \mathcal{X}$
6. The sectional curvature of $\mathcal{X}$ is bounded, *i.e.*, $K_{\min} \leq K_{\mathcal{X}} \leq K_{\max}$.

These assumptions also commonly appear in the previous work [37,14,29,36]. Similar to the previous work [37,14,36] we also define the following constant which is essential in our analysis:

$$\zeta = \begin{cases} \frac{\sqrt{|K_{\min}|}D}{\tanh(\sqrt{|K_{\min}|}D)} & \text{if } K_{\min} < 0 \\ 1 & \text{if } K_{\min} \geq 0 \end{cases}$$

In MASAGA we modify two parts of the original SAGA: (i) since gradients are in different tangent spaces, we use parallel transport to map them into the same tangent plane and then do the variance reduction step (line 6 Alg. 2), and (ii) we use the Exp function to map the update step back into the manifold (line 7 Alg. 2).

Algorithm 2 MASAGA Algorithm

Input: Learning rate η and $x_0 \in \mathcal{M}$
Initialize memory $M^{(0)}$ with gradient of x_0
for $t = 1, 2, 3, \dots$ **do**
  $\hat{\mu} = \frac{1}{n}\sum_{j=1}^{n} M^t[j]$
  Pick i uniformly at random from $\{1 \dots n\}$
  $\nu_t = \nabla f_i(x_t) - \Gamma_{x_0}^{x_t}\left[M^t[i] - \hat{\mu}\right]$
  $x_{t+1} = \mathrm{Exp}_{x_t}(-\eta(\nu_t))$
  Set $M^{t+1}[i] = \Gamma_{x_t}^{x_0}[\nabla f_i(x_t)]$ and $M^{t+1}[j] = M^t[j]$ for all $j \neq i$
end for

3.1 Convergence Analysis

In this section we analyze the convergence of MASAGA considering the above assumptions and we show that it converges linearly. In our analysis, we use the fact that MASAGA's estimation of the full gradient ν_t is unbiased (like SAGA), *i.e.*, $\mathbb{E}[\nu_t] = \nabla f(x_t)$. For simplicity, we use ∇f to denote the Riemannian gradient instead of g_x. We assume that there exists an incremental first-order oracle (IFO) [2] that gets an $i \in \{1, ..., n\}$, and an $x \in \mathcal{X}$, and return $(f_i(x), \nabla f_i(x)) \in (\mathbb{R} \times \mathcal{T}_{\mathcal{M}}(x))$.

Theorem 1. *When each f_i is geodesically L-smooth and f is geodesically μ-strongly convex on the manifold $\mathcal{M}$, the MASAGA algorithm with the constant step size $\eta = \frac{2\mu + \sqrt{\mu^2 - 8\rho(1+\alpha)\zeta L^2}}{4(1+\alpha)\zeta L^2}$ converges linearly while satisfying the following:*

$$\mathbb{E}\left[\mathrm{d}^2(x_t, x^*)\right] \leq (1-\rho)^t \Upsilon^0,$$

where, $\rho = \min\{\frac{\mu^2}{8(1+\alpha)\zeta L^2}, \frac{1}{n} - \frac{1}{\alpha n}\}$, $\alpha > 1$ is a constant, and $\Upsilon^0 = 2\alpha\zeta\eta^2 \sum_{i=1}^{n} \| M^0[i] - \Gamma_{x^*}^{x_0}[\nabla f_i(x^*)] \|^2 + \mathrm{d}^2(x_0, x^*)$ are positive scalars.

Proof. Let $\delta_t = \mathrm{d}^2(x_t, x^*)$. First let us find an upper bound for $\mathbb{E}\left[\|\nu_t\|^2\right]$:

$$\begin{aligned}
\mathbb{E}\left[\|\nu_t\|^2\right] &= \mathbb{E}\left[\|\nabla f_i(x_t) - \Gamma_{x_0}^{x_t}\left[M^t[i] - \hat{\mu}\right]\|^2\right] \\
&= \mathbb{E}\left[\|\nabla f_i(x_t) - \Gamma_{x^*}^{x_t}[\nabla f_i(x^*)] - \Gamma_{x_0}^{x_t}\left[M^t[i] - \Gamma_{x^*}^{x_0}[\nabla f_i(x^*)] - \hat{\mu}\right]\|^2\right] \\
&\leq 2\mathbb{E}\left[\|\nabla f_i(x_t) - \Gamma_{x^*}^{x_t}[\nabla f_i(x^*)]\|^2\right] + 2\mathbb{E}\left[\|\Gamma_{x_0}^{x_t}\left[M^t[i] - \Gamma_{x^*}^{x_0}[\nabla f_i(x^*)] - \hat{\mu}\right]\|^2\right] \\
&\leq 2\mathbb{E}\left[\|\nabla f_i(x_t) - \Gamma_{x^*}^{x_t}[\nabla f_i(x^*)]\|^2\right] + 2\mathbb{E}\left[\|M^t[i] - \Gamma_{x^*}^{x_0}[\nabla f_i(x^*)]\|^2\right] \\
&\leq 2L^2\delta_t + 2\mathbb{E}\left[\|M^t[i] - \Gamma_{x^*}^{x_0}[\nabla f_i(x^*)]\|^2\right]
\end{aligned}$$

The first inequality is due to $(a+b)^2 \leq 2a^2 + 2b^2$ and the second one is from the variance upper bound, *i.e.*, $\mathbb{E}\left[x^2 - \mathbb{E}[x]^2\right] \leq \mathbb{E}\left[x^2\right]$. The last inequality comes from the geodesic Lipschitz smoothness of each f_i.

$$\begin{aligned}
\mathbb{E}[\delta_{t+1}] &\leq \mathbb{E}\left[\delta_t - 2\left\langle \nu_t, \mathrm{Exp}_{x_t}^{-1}(-x^*)\right\rangle + \zeta\eta^2\|\nu_t\|^2\right] \\
&= \delta_t - 2\eta\left\langle \nabla f(x_t), \mathrm{Exp}_{x_t}^{-1}(-x^*)\right\rangle + \zeta\eta^2\mathbb{E}\left[\|\nu_t\|^2\right] \\
&\leq \delta_t - \eta\mu\delta_t + \zeta\eta^2\mathbb{E}\left[\|\nu_t\|^2\right] \\
&\leq (1-\mu\eta)\delta_t + \zeta\eta^2\left[2L^2\delta_t + 2\mathbb{E}\left[\|M^t[i] - \Gamma_{x^*}^{x_0}[\nabla f_i(x^*)]\|^2\right]\right] \\
&= (1 - \mu\eta + 2\zeta L^2\eta^2)\delta_t + 2\zeta\eta^2\Psi_t
\end{aligned}$$

where the first inequality is due to the trigonometric distance bound, the second one is due to the strong convexity of f, and the last one is due to the upper bound for ν_t. Let

$$\Psi_t = \frac{1}{n}\sum_{i=1}^{n} \| M^t[i] - \Gamma_{x^*}^{x_0}\left[\nabla f_i(x^*)\right] \|^2.$$

Now let us define the Lyaponov function:

$$\Upsilon^t = \delta_t + c\,\Psi_t$$

for some $c > 0$. Next we have to find an upper bound for $\mathbb{E}\left[\Psi_{t+1}\right]$.

$$\begin{aligned}
\mathbb{E}\left[\Psi_{t+1}\right] &= \frac{1}{n}(\frac{1}{n}\sum_{i=1}^{n} \| \nabla f_i(x_t) - \Gamma_{x^*}^{x_t}\left[\nabla f_i(x^*)\right] \|^2) + (1-\frac{1}{n})(\frac{1}{n}\sum_{i=1}^{n} \| M^t[i] - \Gamma_{x^*}^{x_0}\left[\nabla f_i(x^*)\right] \|^2) \\
&= \frac{1}{n}(\frac{1}{n}\sum_{i=1}^{n} \| \nabla f_i(x_t) - \Gamma_{x^*}^{x_t}\left[\nabla f_i(x^*)\right] \|^2) + (1-\frac{1}{n})\Psi_t \\
&\leq \frac{L^2}{n}\delta_t + (1-\frac{1}{n})\Psi_t
\end{aligned}$$

where the inequality is due to the geodesic Lipschitz smoothness of f_i. Then, for some positive $\rho \leq 1$ we have the following inequality:

$$\begin{aligned}
\mathbb{E}\left[\Upsilon^{t+1}\right] - (1-\rho)\Upsilon^t \leq (1 - \mu\eta + 2\zeta L^2\eta^2 - (1-\rho) + \frac{cL^2}{n})\delta_t \\
+ (2\zeta\eta^2 - c(1-\rho) + c(1-\frac{1}{n}))\Psi_t
\end{aligned} \tag{1}$$

δ_t and Ψ_t are positive by construction, therefore, if the coefficients of δ_t and Ψ_t in the right hand side of the equation 1 are negative, we would have $\mathbb{E}\left[\Upsilon^{t+1}\right] \leq (1-\rho)\Upsilon^t$. More precisely, we require

$$2\zeta\eta^2 - c(1-\rho) + c(1-\frac{1}{n}) \leq 0 \tag{2}$$

$$1 - \mu\eta + 2\zeta L^2\eta^2 - (1-\rho) + \frac{cL^2}{n} \leq 0 \tag{3}$$

To satisfy 2, we require $\rho \leq \frac{1}{n} - \frac{2\zeta\eta^2}{c}$. If we set $c = 2\alpha n\zeta\eta^2$ for some $\alpha > 1$, then $\rho \leq \frac{1}{n} - \frac{1}{\alpha n}$, which satisfies our requirement.

Now, if we replace the value for c in Inequality 3, we would get:

$$\begin{aligned}
&\rho - \mu\eta + 2\zeta L^2\eta^2 + 2\alpha\zeta L^2\eta^2 \leq 0 \\
&\eta \in (\eta^- = \frac{2\mu - \sqrt{\mu^2 - 8\rho(1+\alpha)\zeta L^2}}{4(1+\alpha)\zeta L^2}, \eta^+ = \frac{2\mu + \sqrt{\mu^2 - 8\rho(1+\alpha)\zeta L^2}}{4(1+\alpha)\zeta L^2})
\end{aligned}$$

To ensure the term under the square root is positive, we also need $\rho < \frac{\mu^2}{8(1+\alpha)\zeta L^2}$. Finally, if we set $\rho = \min\{\frac{\mu^2}{8(1+\alpha)\zeta L^2}, \frac{1}{n} - \frac{1}{\alpha n}\}$ and $\eta = \eta^+$, then we have:

$$\mathbb{E}\left[\Upsilon^{t+1}\right] \leq (1-\rho)^{t+1}\Upsilon^0,$$

where Υ^0 is a scalar. Since $\Psi_t > 0$, $\mathbb{E}\left[\delta_{t+1}\right] \leq \mathbb{E}\left[\Upsilon^{t+1}\right]$ and we get:

$$\mathbb{E}\left[\delta_{t+1}\right] \leq (1-\rho)^{t+1}\Upsilon^0.$$

Corollary 1. *Let* $\beta = \frac{n\mu^2}{8\zeta L^2}$ *and* $\bar{\alpha} = \beta + \sqrt{\frac{\beta^2}{4}+1} > 1$. *If we set,* $\alpha = \bar{\alpha}$ *then we would have* $\rho = \frac{\mu^2}{8(1+\bar{\alpha})\zeta L^2} = \frac{1}{n} - \frac{1}{\bar{\alpha}n}$. *Now, to reach an* ϵ *accuracy,* i.e., $\mathbb{E}\left[\mathrm{d}^2(x_T, x^*)\right] < \epsilon$, *we need :*

$$T \geq (\frac{8(1+\bar{\alpha})\zeta L^2}{\mu^2})\log(\frac{1}{\epsilon}), \tag{4}$$

where T *is the number of necessary iterations.*

Note that this bound is similar to the bound of Zhang *et al*. [36]. To make it clear, notice that $\bar{\alpha} \leq 2\beta + 1$. Therefore, if we plug this upper bound to Inequality 4 we get:

$$T = \mathcal{O}(\frac{(2\beta+2)\zeta L^2}{\mu^2})\log(\frac{1}{\epsilon}) = \mathcal{O}(\frac{n\mu^2}{8\zeta L^2}\frac{\zeta L^2}{\mu^2} + \frac{\zeta L^2}{\mu^2})\log(\frac{1}{\epsilon}) = \mathcal{O}(n + \frac{\zeta L^2}{\mu^2})\log(\frac{1}{\epsilon}).$$

The $\frac{L^2}{\mu^2}$ term in the above bound is the squared condition number that could be prohibitively large in machine learning applications. In contrast, the original SAGA and SVRG algorithms only depend on $\frac{L}{\mu}$ on convex function within linear spaces. In the next section, we improve this bound through non-uniform sampling techniques.

3.2 MASAGA with Non-uniform Sampling

Using non-uniform sampling for stochastic optimization in Euclidean spaces could help us achieve a faster convergence rate [30,20,9]. In this section, we assume that each f_i has its own geodesically L_i-Lipschitz smoothness as opposed to a single geodesic Lipschitz smoothness $L = \max\{L_i\}$. Now, instead of uniformly sampling f_i, we sample f_i with probability $\frac{L_i}{n\bar{L}}$, where $\bar{L} = \frac{1}{n}\sum_{i=1}^n L_i$, and usually $\bar{L} \ll L$. The iteration update is then changed to:

$$x_{t+1} = \mathrm{Exp}_{x_t}(-\eta(\frac{\bar{L}}{L_i}\nu_t)),$$

which keeps the search direction unbiased, *i.e.*, $\mathbb{E}\left[\frac{\bar{L}}{L_i}\nu_t\right] = \nabla f(x_t)$. The following theorem shows the convergence of the new method.

Theorem 2. *When each* f_i *is geodesically* L_i*-smooth and* f *is geodesically* μ*-strongly convex on the manifold* $\mathcal{M}$*, the MASAGA algorithm with the defined non-uniform sampling scheme and the constant step size* $\eta = \frac{2\mu + \sqrt{\mu^2 - 8\rho(\bar{L}+\alpha L)\frac{\zeta}{\gamma}\bar{L}}}{4(\bar{L}+\alpha L)\frac{\zeta}{\gamma}\bar{L}}$ *converges linearly as follows:*

$$\mathbb{E}\left[\mathrm{d}^2(x_t, x^*)\right] \leq (1-\rho)^t\Upsilon^0,$$

where $\rho = \min\{\frac{\gamma\mu^2}{8(1+\alpha)\zeta L\bar{L}}, \frac{\gamma}{n} - \frac{\gamma}{\alpha n}\}$, $\gamma = \frac{\min\{L_i\}}{\bar{L}}$, $L = \max\{L_i\}$, $\bar{L} = \frac{1}{n}\sum_{i=1}^n L_i$, *and* $\alpha > 1$ *is a constant, and* $\Upsilon^0 = \frac{2\alpha\zeta\eta^2}{\gamma}\sum_{i=1}^n \frac{\bar{L}}{L_i}\|M^0[i] - \Gamma_{x^*}^{x_0}\left[\nabla f_i(x^*)\right]\|^2 + \mathrm{d}^2(x_0, x^*)$ *are positive scalars.*

Proof of the above theorem could be found in the supplementary material.

Corollary 2. *Let* $\beta = \frac{n\mu^2}{8\zeta L\bar{L}}$ *and* $\bar{\alpha} = \beta + \sqrt{\frac{\beta^2}{4} + 1} > 1$. *If we set,* $\alpha = \bar{\alpha}$ *then we have* $\rho = \frac{\gamma\mu^2}{8(1+\bar{\alpha})\zeta L\bar{L}} = \frac{\gamma}{n} - \frac{\gamma}{\bar{\alpha}n}$. *Now, to reach an* ϵ *accuracy,* i.e., $\mathbb{E}\left[\mathrm{d}^2(x_T, x^*)\right] < \epsilon$, *we require:*

$$T = \mathcal{O}(n + \frac{\zeta L\bar{L}}{\gamma\mu^2}) \log(\frac{1}{\epsilon}), \tag{5}$$

where T *is the number of the necessary iterations.*

Observe that the number of iterations T in Equality 5 depends on $\bar{L}L$ instead of L^2. When $\bar{L} \ll L$, the difference could be significant. Thus, MASAGA with non-uniform sampling could achieve an ϵ accuracy faster than MASAGA with uniform sampling.

Similarly we can use the same sampling scheme for the RSVRG algorithm [36] and improve its convergence. Specifically, if we change the update of Algorithm 1 of Zhang *et al*. [36] to $x_{t+1}^{s+1} = \mathrm{Exp}_{x_t^{s+1}} -\eta(\frac{\bar{L}}{L_i}\nu_t^{s+1})$, then Theorem 1 and Corollary 1 of Zhang *et al*. [36] would change to the following ones.

Theorem 3. ***[Theorem 1 of [36] with non-uniform sampling]*** *If we use non-uniform sampling in Algorithm 1 of RSVRG [36] and run it with the option I as described in the work, and let*

$$\alpha = \frac{3\zeta\eta\bar{L}^2}{\mu - 2\zeta\eta\bar{L}^2} + \frac{(1 + 4\zeta\eta^2 - 2\eta\mu)^m(\mu - 5\zeta\eta\bar{L}^2)}{\mu - 2\zeta\eta\bar{L}^2} < 1,$$

where m *is the number of the inner loop iterations, then through* S *iterations of the outer loop, we would have:*

$$\mathbb{E}\left[\mathrm{d}^2(\tilde{x}^S, x^*)\right] \leq (\alpha)^S \mathrm{d}^2(\tilde{x}^0, x^*)$$

The above theorem can be proved through a simple modification to the proof of Theorem 1 in RSVRG [36].

Corollary 3. ***[Corollary 1 of [36] with non-uniform sampling]*** *With non-uniform sampling in Algorithm 1 of RSVRG, after* $\mathcal{O}(n + \frac{\zeta\bar{L}^2}{\gamma\mu^2}) \log(\frac{1}{\epsilon})$ *IFO calls, the output* x_a *satisfies*

$$\mathbb{E}\left[f(x_a) - f(x^*)\right] \leq \epsilon$$

Note that through the non-uniform sampling we improved the RSVRG [36] convergence by replacing the L^2 term with a smaller $\bar{L}^2$ term.

4 Experiments: Computing the leading eigenvector

Computing the leading eigenvector is important in many real-world applications. It is widely used in social networks, computer networks, and metabolic networks for community detection and characterization [23]. It can be used to extract a feature that "best" represent the dataset [8] to aid in tasks such as classification, regression, and background subtraction. Furthermore, it can be used in page rank algorithms which require computing the principal eigenvector of the matrix describing the hyperlinks in the web [13]. These datasets can be huge (the web has more than three billion pages [13]). Therefore, speeding up the leading eigenvector computation will have a significant impact on many applications.

We evaluate the convergence of MASAGA by testing it on several datasets through computing the leading eigenvector. The problem can is written as follows:

$$\min_{x^\top x=1} f(x) = -\frac{1}{n} x^\top (\sum_{i=1}^{n} z_i z_i^\top) x, \tag{6}$$

which is a non-convex objective in the Euclidean space $\mathbb{R}^d$, but a convex objective in the Riemannian manifold. Therefore, MASAGA can achieve a linear convergence rate on this problem. We apply our algorithm on the following datasets:

- **Synthetic.** We generate Z as a 1000×100 matrix where each entry is sampled uniformly from $(0, 1)$. To diversify the Lipschitz constants of the individual z_i's, we multiply each z_i with an integer obtained uniformly between 1 and 100.
- **MNIST [17].** We randomly pick 10000 examples corresponding to digits 0-9 resulting in a matrix $Z \in \mathbb{R}^{10{,}000 \times 784}$.
- **Ocean.** We use the ocean video sequence data found in the UCSD background subtraction dataset [18]. It consists of 176 frames, each resized to a 94×58 image.

We compare MASAGA against RSGD [36] and RSVRG [4]. For solving geodesically smooth convex functions on the Riemannian manifold, RSGD and RSVRG achieve sub-linear and linear convergence rates respectively. Since the manifold for Eq. 6 is that of a sphere, we have the following functions:

$$\begin{aligned} P_X(H) &= H - \text{trace}(X^\top H)X, & \nabla_r f(X) &= P_X(\nabla f(X)), \\ \text{Exp}_X(U) &= \cos(||U||)X + \frac{\sin(||U||)}{||U||}U, & \Gamma_y^x(U) &= P_y(U), \end{aligned} \tag{7}$$

where P corresponds to the tangent space projection function, $\nabla_r f$ the Riemannian gradient function, Exp the exponential map function, and Γ the transport function. We evaluate the progress of our algorithms at each epoch t by computing the relative error between the objective value and the optimum, *i.e.*, $\frac{f(x^t)-f^*}{|f^*|}$.

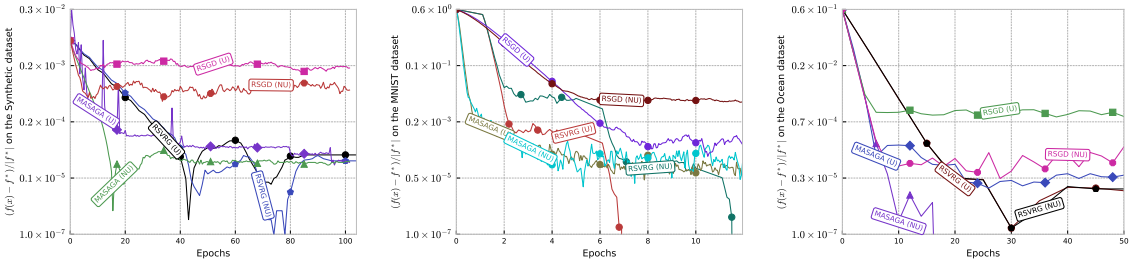

Fig. 1: Comparison of MASAGA (ours), RSVRG, and RSGD for computing the leading eigenvector. The suffix (U) represents uniform sampling and (NU) the non-uniform sampling.

Figure 1 shows that MASAGA is consistently faster than RSGD and RSVRG in the first few epochs. For each algorithm, we perform a grid-search over the learning rates $\{10^{-1}, 10^{-2}, ..., 10^{-9}\}$ and plot the results

(a) Example MNIST images (b) Exact solution (c) MASAGA

Fig. 2: The obtained leading eigenvectors of all MNIST digits.

of the algorithm with the best performance. While it is expected that MASAGA beats RSGD since it has a better convergence rate, the reason MASAGA can outperform RSVRG is that RSVRG needs to occasionally re-compute the full gradient. Furthermore, at each iteration, MASAGA requires a single gradient evaluation instead of two evaluations required by RSVRG. We see in Figure 1 that non-uniform (NU) sampling often leads to faster progress than uniform (U) sampling, which is consistent with the theoretical analysis. In the NU sampling case we sample a vector z_i based on its Lipschitz constant $L_i = ||z_i||^2$. Note that for problems where L_i is not known or costly to compute, we can estimate it by using Algorithm 2 in [30].

(a) MNIST digits (b) MASAGA for digits 1-6

Fig. 3: The obtained leading eigenvectors of the MNIST digits 1-6.

Figures 2 and 3 show the leading eigenvectors obtained for the MNIST dataset. We run MASAGA on $10,000$ images of the MNIST dataset and plot its solution in Figure 2. We see that the exact solution is similar to the solution obtained by MASAGA, which represent the most common strokes among the MNIST digits. Furthermore, we ran MASAGA on 500 images for digits 1-6 independently and plot its solution for each class in Figure 3. Since most digits of the same class have similar shapes and are fairly centered, it is expected that the leading eigenvector would be similar to one of the digits in the dataset.

Figure 4 shows qualitative results comparing MASAGA, RSVRG, and RSGD. We run each algorithm for 20 iterations and plot the results. MASAGA's and RSVRG's results are visually similar to the exact solution. However, the RSGD result is visually different than the exact solution (the difference is in the center-left of the two images).

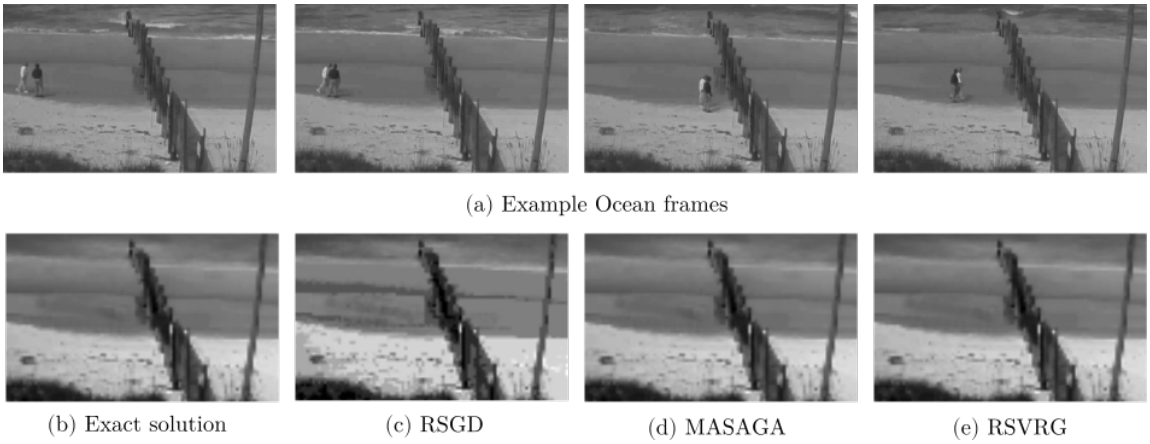

(a) Example Ocean frames

(b) Exact solution (c) RSGD (d) MASAGA (e) RSVRG

Fig. 4: The obtained leading eigenvectors of the ocean dataset after 20 iterations.

5 Conclusion

We introduced MASAGA which is a stochastic variance reduced optimization algorithm for Riemannian manifolds. We analyzed the algorithm and showed that it converges linearly when the objective function is geodesically Lipschitz smooth and strongly convex. We also showed that using non-uniform sampling improves the convergence speed of MASAGA and RSVRG algorithms. Finally, we evaluated our method on a synthetic dataset and two real datasets where we empirically observed linear convergence. The empirical results show that MASAGA outperforms RSGD and is faster than RSVRG in the early iterations. For future work, we plan to extend MASAGA by deriving convergence rates for the non-convex case of geodesic objective functions. We also plan to explore accelerated variance reduction methods and block coordinate descent based methods [25] for Riemannian optimization. Another potential future work of interest is a study of relationships between the condition number of a function within the Euclidean space and its corresponding condition number within a Riemannian manifold, and the effects of sectional curvature on it.

References

1. Absil, P.A., Mahony, R., Sepulchre, R.: Optimization algorithms on matrix manifolds. Princeton University Press (2009)
2. Agarwal, A., Bottou, L.: A lower bound for the optimization of finite sums. arXiv preprint (2014)
3. Bietti, A., Mairal, J.: Stochastic optimization with variance reduction for infinite datasets with finite sum structure. In: Advances in Neural Information Processing Systems. pp. 1622–1632 (2017)
4. Bonnabel, S.: Stochastic gradient descent on riemannian manifolds. IEEE Transactions on Automatic Control **58**(9), 2217–2229 (2013)
5. Cauchy, M.A.: Méthode générale pour la résolution des systèmes d'équations simultanées. Comptes rendus des séances de l'Académie des sciences de Paris **25**, 536–538 (1847)
6. Defazio, A., Bach, F., Lacoste-Julien, S.: Saga: A fast incremental gradient method with support for non-strongly convex composite objectives. Advances in Neural Information Processing Systems (2014)
7. Dubey, K.A., Reddi, S.J., Williamson, S.A., Poczos, B., Smola, A.J., Xing, E.P.: Variance reduction in stochastic gradient langevin dynamics. In: Advances in neural information processing systems. pp. 1154–1162 (2016)

8. Guyon, C., Bouwmans, T., Zahzah, E.h.: Robust principal component analysis for background subtraction: Systematic evaluation and comparative analysis. In: Principal component analysis. InTech (2012)
9. Harikandeh, R., Ahmed, M.O., Virani, A., Schmidt, M., Konečnỳ, J., Sallinen, S.: Stopwasting my gradients: Practical svrg. In: Advances in Neural Information Processing Systems. pp. 2251–2259 (2015)
10. Hosseini, R., Sra, S.: Matrix manifold optimization for gaussian mixtures. In: Advances in Neural Information Processing Systems. pp. 910–918 (2015)
11. Jeuris, B., Vandebril, R., Vandereycken, B.: A survey and comparison of contemporary algorithms for computing the matrix geometric mean. Electronic Transactions on Numerical Analysis **39**(EPFL-ARTICLE-197637), 379–402 (2012)
12. Johnson, R., Zhang, T.: Accelerating stochastic gradient descent using predictive variance reduction. Advances in Neural Information Processing Systems (2013)
13. Kamvar, S., Haveliwala, T., Golub, G.: Adaptive methods for the computation of pagerank. Linear Algebra and its Applications **386**, 51–65 (2004)
14. Kasai, H., Sato, H., Mishra, B.: Riemannian stochastic variance reduced gradient on grassmann manifold. arXiv preprint arXiv:1605.07367 (2016)
15. Konečnỳ, J., Richtárik, P.: Semi-stochastic gradient descent methods. arXiv preprint (2013)
16. Le Roux, N., Schmidt, M., Bach, F.: A stochastic gradient method with an exponential convergence rate for strongly-convex optimization with finite training sets. Advances in Neural Information Processing Systems (2012)
17. LeCun, Y., Bottou, L., Bengio, Y., Haffner, P.: Gradient-based learning applied to document recognition. Proceedings of the IEEE **86**(11), 2278–2324 (1998)
18. Mahadevan, V., Vasconcelos, N.: Spatiotemporal saliency in dynamic scenes. IEEE Transactions on Pattern Analysis and Machine Intelligence **32**(1), 171–177 (2010). https://doi.org/http://doi.ieeecomputersociety.org/10.1109/TPAMI.2009.112
19. Mahdavi, M., Jin, R.: Mixedgrad: An $o(1/t)$ convergence rate algorithm for stochastic smooth optimization. Advances in Neural Information Processing Systems (2013)
20. Needell, D., Ward, R., Srebro, N.: Stochastic gradient descent, weighted sampling, and the randomized kaczmarz algorithm. In: Advances in Neural Information Processing Systems. pp. 1017–1025 (2014)
21. Nemirovski, A., Juditsky, A., Lan, G., Shapiro, A.: Robust stochastic approximation approach to stochastic programming. SIAM Journal on Optimization **19**(4), 1574–1609 (2009)
22. Nesterov, Y.: A method for unconstrained convex minimization problem with the rate of convergence $O(1/k^2)$. Doklady AN SSSR **269**(3), 543–547 (1983)
23. Newman, M.E.: Modularity and community structure in networks. Proceedings of the national academy of sciences **103**(23), 8577–8582 (2006)
24. Nguyen, L., Liu, J., Scheinberg, K., Takáč, M.: Sarah: A novel method for machine learning problems using stochastic recursive gradient. arXiv preprint arXiv:1703.00102 (2017)
25. Nutini, J., Laradji, I., Schmidt, M.: Let's Make Block Coordinate Descent Go Fast: Faster Greedy Rules, Message-Passing, Active-Set Complexity, and Superlinear Convergence. ArXiv e-prints (Dec 2017)
26. Petersen, P., Axler, S., Ribet, K.: Riemannian geometry, vol. 171. Springer (2006)
27. Polyak, B.T., Juditsky, A.B.: Acceleration of stochastic approximation by averaging. SIAM Journal on Control and Optimization **30**(4), 838–855 (1992)
28. Robbins, H., Monro, S.: A stochastic approximation method. Ann. Math. Statist. **22**(3), 400–407 (09 1951). https://doi.org/10.1214/aoms/1177729586, http://dx.doi.org/10.1214/aoms/1177729586
29. Sato, H., Kasai, H., Mishra, B.: Riemannian stochastic variance reduced gradient. arXiv preprint arXiv:1702.05594 (2017)
30. Schmidt, M., Babanezhad, R., Ahmed, M., Defazio, A., Clifton, A., Sarkar, A.: Non-uniform stochastic average gradient method for training conditional random fields. In: Artificial Intelligence and Statistics. pp. 819–828 (2015)
31. Shalev-Schwartz, S., Zhang, T.: Stochastic dual coordinate ascent methods for regularized loss minimization. Journal of Machine Learning Research **14**, 567–599 (2013)
32. Sun, J., Qu, Q., Wright, J.: Complete dictionary recovery over the sphere. In: Sampling Theory and Applications (SampTA), 2015 International Conference on. pp. 407–410. IEEE (2015)

33. Udriste, C.: Convex functions and optimization methods on Riemannian manifolds, vol. 297. Springer Science & Business Media (1994)
34. Wager, S., Fithian, W., Wang, S., Liang, P.S.: Altitude training: Strong bounds for single-layer dropout. In: Advances in Neural Information Processing Systems. pp. 100–108 (2014)
35. Wiesel, A.: Geodesic convexity and covariance estimation. IEEE Transactions on Signal Processing **60**(12), 6182–6189 (2012)
36. Zhang, H., Reddi, S.J., Sra, S.: Riemannian svrg: fast stochastic optimization on riemannian manifolds. In: Advances in Neural Information Processing Systems. pp. 4592–4600 (2016)
37. Zhang, H., Sra, S.: First-order methods for geodesically convex optimization. In: Conference on Learning Theory. pp. 1617–1638 (2016)
38. Zhang, T., Yang, Y.: Robust principal component analysis by manifold optimization. arXiv preprint arXiv:1708.00257 (2017)
39. Zhao, P., Zhang, T.: Stochastic optimization with importance sampling for regularized loss minimization. In: international conference on machine learning. pp. 1–9 (2015)
40. Ziller, W.: Riemannian manifolds with positive sectional curvature. In: Geometry of manifolds with non-negative sectional curvature, pp. 1–19. Springer (2014)

6 Appendix

6.1 Proof of Theorem 2

Proof. Let $\delta_t = \mathrm{d}^2(x_t, x^*)$. First let us find an upper bound for $\mathbb{E}\left[\|\frac{\bar{L}}{L_i}\nu_t\|^2\right]$:

$$\begin{aligned}
\mathbb{E}\left[\|\frac{\bar{L}}{L_i}\nu_t\|^2\right] &= \mathbb{E}\left[(\frac{\bar{L}}{L_i})^2\|\nabla f_i(x_t) - \Gamma_{x_0}^{x_t}\left[M^t[i] - \hat{\mu}\right]\|^2\right] \\
&= \mathbb{E}\left[(\frac{\bar{L}}{L_i})^2\|\nabla f_i(x_t) - \Gamma_{x^*}^{x_t}\left[\nabla f_i(x^*)\right] - \Gamma_{x_0}^{x_t}\left[M^t[i] - \Gamma_{x^*}^{x_0}\left[\nabla f_i(x^*)\right] - \hat{\mu}\right]\|^2\right] \\
&\leq 2\mathbb{E}\left[(\frac{\bar{L}}{L_i})^2\|\nabla f_i(x_t) - \Gamma_{x^*}^{x_t}\left[\nabla f_i(x^*)\right]\|^2\right] + 2\mathbb{E}\left[\|(\frac{\bar{L}}{L_i})(\Gamma_{x_0}^{x_t}\left[M^t[i] - \Gamma_{x^*}^{x_0}\left[\nabla f_i(x^*)\right] - \hat{\mu}\right])\|^2\right] \\
&\leq 2\mathbb{E}\left[(\frac{\bar{L}}{L_i})^2\|\nabla f_i(x_t) - \Gamma_{x^*}^{x_t}\left[\nabla f_i(x^*)\right]\|^2\right] + 2\mathbb{E}\left[(\frac{\bar{L}}{L_i})^2\|M^t[i] - \Gamma_{x^*}^{x_0}\left[\nabla f_i(x^*)\right]\|^2\right] \\
&\leq 2\mathbb{E}\left[(\frac{\bar{L}}{L_i})^2 L_i^2\delta_t\right] + 2\mathbb{E}\left[(\frac{\bar{L}}{L_i})^2\|M^t[i] - \Gamma_{x^*}^{x_0}\left[\nabla f_i(x^*)\right]\|^2\right] \\
&= 2\bar{L}^2\delta_t + 2\mathbb{E}\left[(\frac{\bar{L}}{L_i})^2\|M^t[i] - \Gamma_{x^*}^{x_0}\left[\nabla f_i(x^*)\right]\|^2\right] \\
&= 2\bar{L}^2\delta_t + 2\frac{1}{n}\sum_{i=1}^{n}(\frac{\bar{L}}{L_i})\|M^t[i] - \Gamma_{x^*}^{x_0}\left[\nabla f_i(x^*)\right]\|^2
\end{aligned}$$

The first inequality is due to $(a+b)^2 \leq 2a^2 + 2b^2$ and the second one is from the variance upper bound, i.e., $\mathbb{E}\left[x^2 - \mathbb{E}\left[x\right]^2\right] \leq \mathbb{E}\left[x^2\right]$. The last inequality comes from the Lipschitz smoothness of each f_i. The last equality is due to fact that we sample each f_i with probability $\frac{L_i}{n\bar{L}_i}$.

$$\begin{aligned}
\mathbb{E}\left[\delta_{t+1}\right] &\leq \mathbb{E}\left[\delta_t - 2\left\langle \frac{\bar{L}}{L_i}\nu_t, \mathrm{Exp}_{x_t}^{-1}(-x^*)\right\rangle + \zeta\eta^2\|\frac{\bar{L}}{L_i}\nu_t\|^2\right] \\
&= \delta_t - 2\eta\left\langle \nabla f(x_t), \mathrm{Exp}_{x_t}^{-1}(-x^*)\right\rangle + \zeta\eta^2\mathbb{E}\left[\|\frac{\bar{L}}{L_i}\nu_t\|^2\right] \\
&\leq \delta_t - \eta\mu\delta_t + \zeta\eta^2\mathbb{E}\left[\|\frac{\bar{L}}{L_i}\nu_t\|^2\right] \\
&\leq (1-\mu\eta)\delta_t + \zeta\eta^2\left[2\bar{L}^2\delta_t + 2\frac{1}{n}\sum_{i=1}^{n}(\frac{\bar{L}}{L_i})\|M^t[i] - \Gamma_{x^*}^{x_0}\left[\nabla f_i(x^*)\right]\|^2\right] \\
&= (1-\mu\eta+2\zeta\bar{L}^2\eta^2)\delta_t + 2\zeta\eta^2\Psi_t
\end{aligned}$$

where the first inequality is due to the trigonometric distance bound, the second one is due to strong convexity of f, and the last one is due to upper bound for ν_t. Let

$$\Psi_t = \frac{1}{n}\sum_{i=1}^{n}(\frac{\bar{L}}{L_i})\|M^t[i] - \Gamma_{x^*}^{x_0}\left[\nabla f_i(x^*)\right]\|^2.$$

Now let us define the Lyaponov function:

$$\Upsilon^t = \delta_t + c\,\Psi_t$$

for some $c > 0$. Next we have to find an upper bound for $\mathbb{E}\left[\Psi_{t+1}\right]$.

$$\begin{aligned}
\mathbb{E}\left[\Psi_{t+1}\right] &= \frac{1}{n}(\sum_{i=1}^{n}\frac{L_i}{n\bar{L_i}}(\frac{\bar{L}}{L_i})\|\nabla f_i(x_t) - \Gamma_{x^*}^{x_t}\left[\nabla f_i(x^*)\right]\|^2) + (\frac{1}{n}\sum_{i=1}^{n}(1-\frac{L_i}{n\bar{L_i}})\|M^t[i] - \Gamma_{x^*}^{x_0}\left[\nabla f_i(x^*)\right]\|^2) \\
&= \frac{1}{n}(\frac{1}{n}\sum_{i=1}^{n}\|\nabla f_i(x_t) - \Gamma_{x^*}^{x_t}\left[\nabla f_i(x^*)\right]\|^2) + (1-\frac{\gamma}{n})\Psi_t \\
&\leq \frac{1}{n}(\frac{1}{n}\sum_{i=1}^{n}L_i^2\delta_t) + (1-\frac{\gamma}{n})\Psi_t \\
&\leq \frac{L\bar{L}}{n}\delta_t + (1-\frac{\gamma}{n})\Psi_t
\end{aligned}$$

where $\gamma = \frac{\min\{L_i\}}{\bar{L}}$ .The first inequality is due to geodesic Lipschitz smoothness of f_i. Then for some positive $\rho \leq 1$ we have the following inequality:

$$\begin{aligned}
\mathbb{E}\left[\Upsilon^{t+1}\right] - (1-\rho)\Upsilon^t \leq (1-\mu\eta+2\zeta\bar{L}^2\eta^2 - (1-\rho) + \frac{cL\bar{L}}{n})\delta_t \\
+ (2\zeta\eta^2 - c(1-\rho) + c(1-\frac{\gamma}{n}))\Psi_t
\end{aligned} \tag{8}$$

So if the coefficients of δ_t and Ψ_t in the right hand side of the equation 8 are negative, we have $\mathbb{E}\left[\Upsilon^{t+1}\right] \leq (1-\rho)\Upsilon^t$. More precisely, we need

$$2\zeta\eta^2 - c(1-\rho) + c(1-\frac{\gamma}{n}) \leq 0 \tag{9}$$

$$1 - \mu\eta + 2\zeta\bar{L}^2\eta^2 - (1-\rho) + \frac{cL\bar{L}}{n} \leq 0 \tag{10}$$

To satisfy 9, we have:

$$2\zeta\eta^2 + c\rho - \frac{c\gamma}{n} \leq 0$$
$$\rho \leq \frac{\gamma}{n} - \frac{2\zeta\eta^2}{c}$$

let $c = \frac{2\alpha n\zeta\eta^2}{\gamma}$ for some $\alpha > 1$, then $\rho \leq \frac{\gamma}{n} - \frac{\gamma}{\alpha n}$.

Now, we replace the value for c in the 10, we get:

$$\rho - \mu\eta + 2\zeta\bar{L}^2\eta^2 + 2\alpha\frac{\zeta}{\gamma}L\bar{L}\eta^2 \leq 0$$
$$\eta \in (\eta^- = \frac{2\mu - \sqrt{\mu^2 - 8\rho(\bar{L}+\alpha L)\frac{\zeta}{\gamma}\bar{L}}}{4(\bar{L}+\alpha L)\frac{\zeta}{\gamma}L^2}, \eta^+ = \frac{2\mu + \sqrt{\mu^2 - 8\rho(\bar{L}+\alpha L)\frac{\zeta}{\gamma}\bar{L}}}{4(\bar{L}+\alpha L)\frac{\zeta}{\gamma}\bar{L}})$$

To get the term under square root be positive, we need that $\rho < \frac{\mu^2}{8(\bar{L}+\alpha L)\frac{\zeta}{\gamma}\bar{L}} < \frac{\mu^2}{8(1+\alpha)\frac{\zeta}{\gamma}L\bar{L}}$ holds. Finally if we set $\rho = \min\{\frac{\gamma\mu^2}{8(1+\alpha)\zeta L\bar{L}}, \frac{\gamma}{n} - \frac{\gamma}{\alpha n}\}$ and $\eta = \eta^+$, then we have:

$$\mathbb{E}\left[\Upsilon^{t+1}\right] \leq (1-\rho)^{t+1}\Upsilon^0$$

where Υ^0 is a scalar. Since $\Psi_t > 0$, then $\mathbb{E}\left[\delta_{t+1}\right] \leq \mathbb{E}\left[\Upsilon^{t+1}\right]$ and we get:

$$\mathbb{E}\left[\delta_{t+1}\right] \leq (1-\rho)^{t+1}\Upsilon^0$$